

RESEARCH PAPER

Nedd4-1 regulates human sodium-dependent vitamin C transporter-2 functional expression in neuronal and epithelial cells

Trevor Teafatiller^a, Oasis Perez^a, Masashi Kitazawa^b, Anshu Agrawal^a, Veedamali S. Subramanian^{a,*}

^a Department of Medicine, University of California, Irvine, California, USA

^b Department of Environmental and Occupational Health, University of California, Irvine, California, USA

Received 12 May 2023; received in revised form 12 June 2023; accepted 5 July 2023

Abstract

The ubiquitin-proteasomal pathway regulates the functional expression of many membrane transporters in a variety of cellular systems. Nothing is currently known about the role of ubiquitin E3 ligase, neural precursor cell-expressed developmentally down-regulated gene 4 (Nedd4-1) and the proteasomal degradation pathway in regulating human vitamin C transporter-2 (hSVCT2) in neuronal cells. hSVCT2 mediates the uptake of ascorbic acid (AA) and is the predominantly expressed vitamin C transporter isoform in neuronal systems. Therefore, we addressed this knowledge gap in our study. Analysis of mRNA revealed markedly higher expression of Nedd4-1 in neuronal samples than that of Nedd4-2. Interestingly, Nedd4-1 expression in the hippocampus was higher in patients with Alzheimer's disease (AD) and age-dependently increased in the J20 mouse model of AD. The interaction of Nedd4-1 and hSVCT2 was confirmed by coimmunoprecipitation and colocalization. While the coexpression of Nedd4-1 with hSVCT2 displayed a significant decrease in AA uptake, siRNA-mediated knockdown of Nedd4-1 expression up-regulated the AA uptake. Further, we mutated a classical Nedd4 protein interacting motif ("PPXY") within the hSVCT2 polypeptide and observed markedly decreased AA uptake due to the intracellular localization of the mutated hSVCT2. Also, we determined the role of the proteasomal degradation pathway in hSVCT2 functional expression in SH-SY5Y cells and the results indicated that the proteasomal inhibitor (MG132) significantly up-regulated the AA uptake and hSVCT2 protein expression level. Taken together, our findings show that the regulation of hSVCT2 functional expression is at least partly mediated by the Nedd4-1 dependent ubiquitination and proteasomal pathways.

© 2023 Elsevier Inc. All rights reserved.

Keywords: Vitamin C; ascorbic acid; transporter; ubiquitination; proteasomal pathway.

1. Introduction

Vitamin C (ascorbic acid; AA) is a naturally occurring micronutrient in some foods and is also available as a common dietary supplement. Humans cannot synthesize this water-soluble vitamin *de novo* or maintain reserves in the body, thus regular ingestion of vitamin C-rich foods or access to other external sources is essential. Scurvy and increased risk of certain cancers are amongst the many notable conditions linked to vitamin C deficiency. Moreover, studies have reported that vitamin C provides protection against the onset and progression of Alzheimer's disease (AD) [1]. Several studies have examined the role of vitamin C in AD, especially its capacity to reduce oxidative stress that is a major contributor of AD pathology [2]. Neuronal AA uptake occurs through a Na⁺-dependent carrier-mediated mechanism via sodium-dependent vitamin C transporter-2 (SVCT2, the product of the *SLC23A2* gene) [3–6] and this transport protein's functional expression is highly

regulated. Although the vitamin C transport system has been linked to neurodegenerative conditions, what remains unknown are the underlying molecular mechanisms that lead to a deficiency of vitamin C in neurodegenerative diseases and how this deficiency increases inflammation and accelerates pathogenesis.

Previous findings have highlighted the importance of ubiquitination in the expression of both transporters and solute carriers [7]. Ubiquitination is a crucial process in modulating the distribution of intracellular proteins. Ubiquitin itself is a small, highly conserved protein composed of 76 amino acids, and is expressed in all eukaryotic cells. Ubiquitination is a post-translational modification that facilitates covalent conjugation of ubiquitin (Ub) to the lysine (Lys) residue of target proteins [8,9]. The process of ubiquitinating substrates involves the coordinated action of E1, E2, and E3 enzymes. Collectively, these E3 ligases transfer ubiquitin to a specific protein substrate. Binding of one ubiquitin moiety to a substrate's Lys is called mono-ubiquitination, and mono-ubiquitination of many Lys residues of a protein results in multiubiquitination or poly-ubiquitination. The ubiquitination configuration determines the nature of the trajectory of the process including cell cycle progression, DNA repair, transcription,

* Corresponding author at: Veedamali S. Subramanian, 821 Health Science Road, Irvine, CA, USA. Tel.: +949-824-3084

E-mail address: vsubrama@uci.edu (V.S. Subramanian).

apoptosis, endocytosis, protein degradation, and intracellular trafficking [10,11]. The neural precursor cell-expressed developmentally down-regulated 4 (Nedd4) family of E3 ubiquitin ligases includes Nedd4-1 and Nedd4-2. Both Nedd4-1 and Nedd4-2 are involved in the ubiquitination of several mammalian transporters in various cellular systems [12–17]. Further, Nedd4-1 plays a crucial role in neuronal development [18,19] and its importance in neurodegeneration has been recognized in recent years [20–25]. A classical Nedd4 protein interacting motif (“PPXY”) allows specified association with protein substrates [14,26]. Interestingly, this motif is present in SVCT transporters and is conserved across species (human, rat, and mouse). Additionally, Persaud et al. [27] identified through proteomic analysis that hSVCT2 interacts with Nedd4-1 and also demonstrated that SVCT2 expression is suppressed in AD brain [28]. Previous studies showed that Nedd4-1 has a role in AD brain, where it mediates synaptic alterations induced by amyloid-beta ($A\beta$) by reducing surface AMPA receptors (AMPA-Rs) density [22,25]. In addition, studies have also shown that the proteasomal degradation pathway plays a role in regulating transporter function [13,29,30].

Understanding the relationship between Nedd4-1 and hSVCT2 has great potential to provide insight as to the implications of interaction given the known functional properties of each of these proteins. The outcomes from this study demonstrate that Nedd4-1 expression in neuronal samples was higher than that of Nedd4-2. Further, the coexpression of Nedd4-1 with hSVCT2 decreased the AA uptake. Conversely, Nedd4-1 knockdown up-regulated the AA uptake. In addition, the proteasomal degradation pathway was involved in hSVCT2 functional expression in SH-SY5Y cells. Overall, Nedd4-1 may be playing a role in neuronal vitamin C deficiency in AD by reducing the expression of hSVCT2.

2. Materials and methods

2.1. Reagents

Radiosynthesis of Ascorbic acid, L-[1- ^{14}C] (2.8–10 mCi/mmol, radiochemical purity >98%) was completed by American Radiolabeled Chemicals/PerkinElmer Inc. (St. Louis, MO/Boston, MA, USA). Both SH-SY5Y and HEK-293 are authenticated cell lines, human-derived neuroblastoma and embryonic kidney, respectively. DMEM/F12 and EMEM cell culture media were procured from the American Type Culture Collection (ATCC; Manassas, VA, USA). Carbobenzoyl-L-leucyl-L-leucyl-L-leucine (MG132) was obtained from Sigma (St. Louis, MO, USA). pCI HA-Nedd4-1 plasmid was obtained from Addgene (Watertown, MA, USA). Oligonucleotide primers designed for RT-qPCR and site-directed mutational analysis were synthesized by Integrated DNA Technologies, Inc. (San Diego, CA, USA). Additional reagents and other materials for molecular biology applications were bought from commercial vendors.

2.2. Cell culture and transfection

Cells were maintained in a SC05A air jacketed cell incubator (Sheldon Manufacturing, Inc., Cornelius, OR, USA) with a 5% CO_2 -95% O_2 atmosphere at 37°C and passive humidification. SH-SY5Y cells were cultured in DMEM/F12 with 20% FBS (Gemini Bio Products, West Sacramento, CA, USA) and HEK-293 cells were cultured in EMEM with 10% FBS. Both growth media were also supplemented with 1% Pen-Strep (10,000 IU/mL, 10 mg/mL; Thermo Fisher Scientific, CA, USA) to prevent bacterial contamination. Cell expansion occurred in tissue culture-treated T75-cm² flasks, while 12-well flat bottom plates (Corning Life Sciences, Tewksbury, MA, USA) and glass bottom petri-dishes (MatTek, Ashland, MA, USA) were used to cultivate subcultures for cell-based experiments and

high resolution imaging. Media changes were conducted regularly and once cell confluence reached approximately 90% of the culture vessel surface area, cells were transiently transfected using plasmid DNA (3 μ g) complexed with Lipofectamine 2,000 (3 μ l; Invitrogen, Carlsbad, CA, USA) applied to each well/dish. The cells were subjected for analysis 48h post-transfection.

2.3. Human and mouse hippocampus tissue preparation

The mutant mouse strain, J20, comes from a C57BL/6J genetic background and has mutations in amyloid precursor protein (APP; APP KM670/671NL (Swedish), APP V717F (Indiana)) [31]. J20 mice are a common familial Alzheimer's disease (AD) model that features elevated $A\beta$ levels in hippocampal neurons that develop at approximately 6 weeks of age. The previously described hippocampus extraction protocol [28] was approved by the University of California, Irvine (UCI), Institutional Animal Care and Use Committee (IACUC). Samples of human hippocampus tissue from nondemented and AD patients were supplied by the Alzheimer's Disease Research Center (ADRC) at the UCI Institute for Memory Impairments and Neurological Disorders (UCI MIND) following protocol encompassing brain autopsy consent and de-identification methods that received authorization from UCI's Institutional Review Board (IRB). Proven procedure for total RNA isolation was applied to the human and mouse tissue samples.

2.4. Coimmunoprecipitation and Western blot analysis

HA-Nedd4-1 and hSVCT2-YFP were cotransfected into HEK-293 cells. After 48h of transfection, the cells were washed with cold phosphate buffered saline (PBS) and lysed using the Capturem IP and Co-IP Kit (Takara Biosciences, San Diego, CA, USA) following the manufacturer's instructions. Cleared supernatant was separated from cell lysates after centrifugation at 17,000g for 10min at 4°C. 600 μ l of lysate was incubated with 5 μ g/ml of antihemagglutinin (HA) polyclonal antibodies (Invitrogen, Carlsbad, CA, USA) for 40min at room temperature (RT). After incubation, ~500 μ l of sample was added onto the spin column and then briefly centrifuged at RT. The spin column was then washed with the wash buffer provided in the kit and centrifuged. Finally, 30 μ l of elution buffer was added to the spin column to release the immunoprecipitated protein complexes by centrifugation. These complexes were incubated with NuPAGE sample buffer and reducing agent in a 95°C water bath for 3min and samples were then separated using NuPAGE 10-well 10% Bis-Tris minigel (Invitrogen) and transferred onto Immobilon-FL PVDF membrane (Sigma Millipore, Temecula, CA, USA). The membranes were blocked at RT in LI-COR blocking buffer and incubated with anti-GFP monoclonal primary antibody (1:1,000 dilution; Takara Biosciences, CA, USA) and subsequently probed with labeled IRDye secondary antibody, antimouse 800 (1:30,000 dilution; LI-COR Biosciences, Lincoln, NE, USA). Separation of Nedd4-1 siRNA or MG132 treated or HA-Nedd4-1 and hSVCT2-YFP cotransfected cell line total protein samples (30–60 μ g) was accomplished with Invitrogen NuPAGE 4–12% Bis-Tris minigels (Invitrogen) and transferred to Immobilon-FL PVDF membrane. Anti-hSVCT2 (1:1000 dilution; previously characterized [32]), anti-Nedd4-1 (1:300; Proteintech, IL, USA), anti-GFP (1:1000 dilution; Takara Biosciences), anti-HA (1:1000 dilution; Invitrogen) and anti- β -actin antibodies (1:5000; Thermo Fisher, CA, USA) served as primary antibodies that were subsequently probed with labeled IRDye secondary antibodies, antimouse 680 and antirabbit 800 (1:30,000 dilutions; LI-COR Biosciences). The relative bands captured and intensities of individual proteins were calculated with a LI-COR Odyssey infrared imaging platform.

2.5. Confocal microscopy

Ninety percent confluent (subconfluent) monolayers of HEK-293 cells cultured in glass bottom petri dishes were transiently transfected with combinations of hSVCT2-DsRed, Nedd4-1-GFP (a gift from Dr. Peter Snyder, University of Iowa), hSVCT2-YFP, hSVCT2-[PPWYAAAA]-YFP and DsRed-ER constructs (2 μ g each) that were complexed with Lipofectamine 2000 (2 μ l; Invitrogen). By utilizing a Nikon Eclipse Ti2 confocal microscope with 60X magnification (Nikon 60X oil lens), we were able to image the live cells simultaneously overexpressing genes to perform colocalization studies. The accompanying Nikon imaging software (NIS) was used to image GFP/YFP at 488nm and DsRed at 555nm.

2.6. Small interfering RNA (siRNA) analysis

HEK-293 cells in 12-well plates were grown up to 90% confluence before being transiently transfected with lipofectamine RNAiMAX reagent (2 μ l per well; Invitrogen) and either Nedd4-1 siRNA (20nM; Ambion, Austin, CA, USA) or negative control (scrambled) siRNA (20nM). cDNA was synthesized from total RNA extracted from the transfected cells after 48h of further culture using TRIzol reagent (Invitrogen) for use in RT-qPCR to determine the knockdown potency of the siRNA targeting Nedd4-1 expression. siRNA transfection preparations were also used to perform ¹⁴C-AA uptake analysis in separate batches of HEK-293 cells.

2.7. RT-qPCR analysis

Cultured cells (HEK-293, SH-SY5Y), and human (nondemented, AD) or mouse (C57BL/6J, J20) hippocampus tissue were lysed using TRIzol reagent to extract total RNA [28,32]. The total RNA from each sample was then used with the iScript cDNA Synthesis Kit (Bio-Rad, Hercules, CA) reagents to make cDNA template. Each amplicon was subjected to RT-qPCR with corresponding primers for human (h)SVCT2, hNedd4-1, hNedd4-2, h β -actin, mouse (m)Nedd4-1, mNedd4-2, and m β -actin primers (hNedd4-1-F-5'-CCAGTTGGGAAGAAAAACA-3'; R-5'-ATTCAGATGGCTGGTCC-3', hNedd4-2-F-5'-GGGTGGTGAGGAACCAACG-3'; R-5'-TGATAGGTCGAGTCCAAGTTGT-3', h β -actin-F-5'-CATCCTGCGTCTGGACT-3'; R-5'-TAATGTCACGCACGATTTCC-3', mNedd4-1-F-5'-TCGGA GGACGAGGTATGGG-3'; R-5'-GGTACGGATCAGCACTGAACA-3', mNedd4-2-F-5'-CACGGGTGGTGAGGAATCC-3'; R-5'-GCCGAGTCCAAGTTG TGGT-3', and m β -actin-F-5'-ATCCTTCTCCCTGGA-3'; R-5'-TTCATGGATGCCACAGGA-3') in iQ SYBR Green Supermix (Bio-Rad). Output data from a CFX96 Touch Real-Time PCR Detection System (Bio-Rad) was normalized relative to a housekeeping gene (β -actin) and then computed through a relative relationship method established by the manufacturer.

2.8. Site-directed mutagenesis

hSVCT2-YFP DNA template, oligonucleotide primers containing a mutated sequence as underlined (sense-F-5'-GAAGATGTTGCTGCCGGCCCTGTGTATA-3'; antisense-R-5'-TATACACAGGGCCGGCAGCAACATCTTC-3') and reagents from a QuikChange XL Site-Directed Mutagenesis Kit (Agilent Technologies, Inc., Santa Clara, CA) were used for site-directed mutation analysis. The site-specific mutation resulted in the incorporation of the mutant oligonucleotide primers into the open reading frame (ORF) of the hSVCT2 PPWY motif. DNA sequencing (Azenta Life Sciences, La Jolla, CA, USA) verified the identity of the mutated plasmid.

2.9. Uptake studies

Cells (SH-SY5Y and HEK-293) were cultured on 12-well plates to 90% confluence before treatment (MG132) or transient transfection with different plasmids and then washed with warm Krebs-Ringer (KR) buffer. Next, KR buffer containing labeled or unlabeled plus labeled ¹⁴C-AA (0.1 μ Ci) was added to the wells while the bottom of the plate was submerged in a 37°C water bath. After a 30min incubation period, the solution in each well was aspirated and a wash with ice-cold KR buffer was applied to stop the reaction. NaOH solution was then added before the cells were baked at 85°C in an air incubator for 15min, and the cell lysate was then neutralized with HCl before samples were taken for recording the ionizing radiation by a LS6500 analyzer (Beckman Coulter, Brea, CA) as described previously [6,28].

2.10. Statistical analysis

The Student's t-test ($P < .05$) provided the basis for statistical significance. All data including from vitamin uptake analysis, Western blot, and RT-qPCR are presented as mean \pm SEM in percentage relative to controls from a minimum of three experimental runs. Additionally, *in vitro* experiments were completed using multiple passages of cells, and human and mouse studies were done with the necessary sample size to maintain statistical significance. Live cell confocal imaging was confirmed by triplicate sample preparations.

3. Results

3.1. Nedd4-1 and Nedd4-2 mRNA expression in hippocampus and SH-SY5Y cells

Expression of Nedd4-1 and Nedd4-2 mRNA in normal human hippocampus (Fig. 1A), human-derived neuroblastoma SH-SY5Y cells (Fig. 1B), and normal mouse hippocampus (Fig. 1C) was determined by RT-qPCR. The results revealed that Nedd4-1 expression was markedly higher than that of Nedd4-2 in all three systems tested.

3.2. Nedd4-1 expression up-regulated in human and mouse AD hippocampus

Previous studies have shown the role of Nedd4-1 in AD [25]. Therefore, we determined the status of Nedd4-1 mRNA expression in human and mouse AD hippocampus. We observed a significant ($P < .05$) increase of hNedd4-1 mRNA expression in the hippocampus from AD patients (Fig. 2A). Interestingly, we also found that the expression of mNedd4-1 in J20 mouse hippocampus was markedly increased as a function of age for up to 19 months relative to age matched controls (Fig. 2B).

3.3. Nedd4-1 interacts with hSVCT2 in HEK-293 cells

Persaud et al. [27] identified that hSVCT2 interacts with Nedd4-1 by proteomic analysis. The interaction between hNedd4-1 and hSVCT2 was determined by coimmunoprecipitation. To do this, we cotransfected HA-Nedd4-1 and hSVCT2-YFP constructs into HEK-293 cells and included mock transfected controls that were then immunoprecipitated using anti-HA antibodies. Western blot analysis using anti-GFP antibodies revealed the presence of hSVCT2 in HA-Nedd4-1 and hSVCT2-YFP transfected cells, and absence of hSVCT2 in HEK-293 mock transfected control cells (Fig. 3Ai). In addition, the lysates of HEK-293 cells transiently coexpressing HA-Nedd4-1 and hSVCT2-YFP constructs were subjected to Western

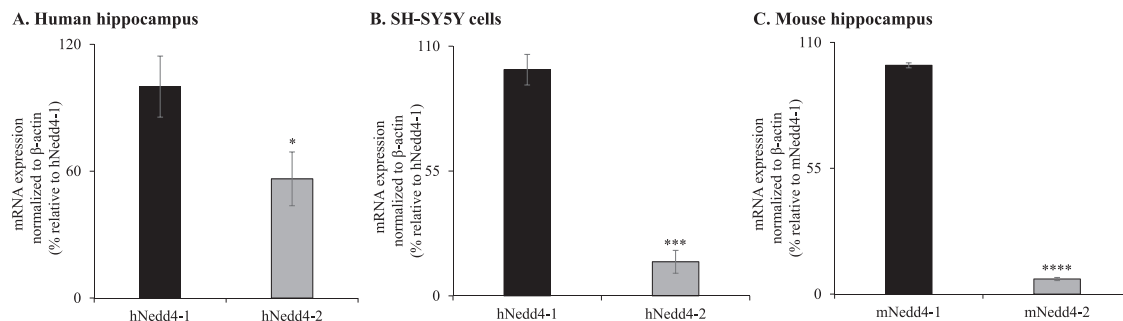


Fig. 1. Nedd4-1 and Nedd4-2 mRNA are differentially expressed in hippocampus and SH-SY5Y cells. Total RNA was analyzed by RT-qPCR to determine Nedd4-1 and Nedd4-2 mRNA expression levels in human hippocampus (A), SH-SY5Y cells (B) and mouse hippocampus (C). Data are mean \pm SEM of at least 3 individual cell culture preparations or multiple human and mouse samples ($n=3-6$). * $P<.05$; *** $P<.001$; **** $P<.0001$.

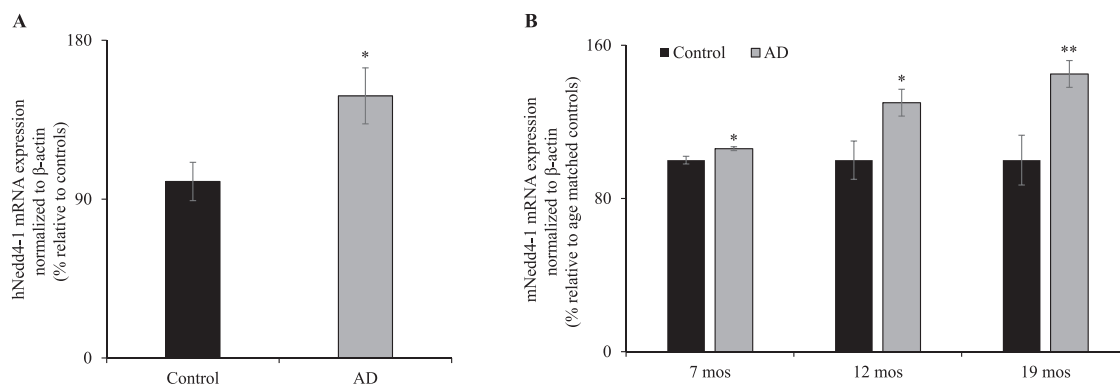


Fig. 2. Upregulation of Nedd4-1 mRNA expression in the hippocampus of AD patients and J20 mice. The levels of Nedd4-1 mRNA expression were quantified by RT-qPCR in human AD and healthy controls (A) and different age (7, 12, and 19 months) group J20 mouse (B) hippocampus samples. Data are mean \pm SEM of at least three separate experiments ($n=3-5$). * $P<.05$; ** $P<.01$.

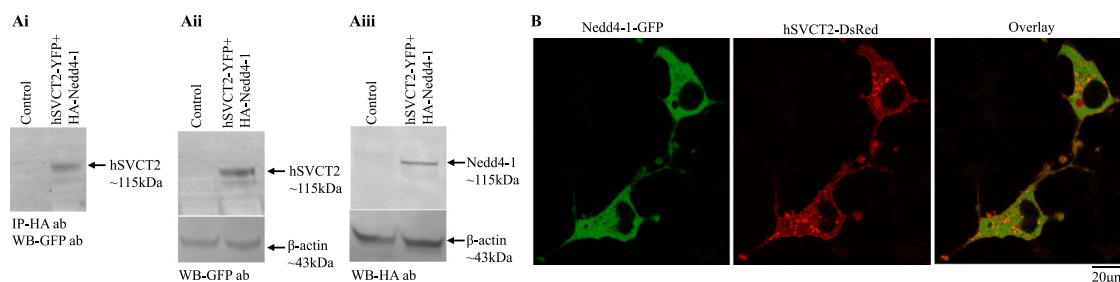


Fig. 3. Nedd4-1 interacts with hSVCT2 in HEK-293 cells. (Ai) HEK-293 cells transiently cotransfected with HA-Nedd4-1 and hSVCT2-YFP were lysed and immunoprecipitated (IP) using anti-HA polyclonal antibodies and Western blots (WB) were developed with anti-GFP monoclonal antibodies. Immunoprecipitate obtained from mock transfected HEK-293 cells served as control. HEK-293 cells transiently coexpressing HA-Nedd4-1 and hSVCT2-YFP cell lysates were subjected to Western blot analysis and developed with anti-GFP antibodies (Aii) or anti-HA antibodies (Aiii). (B) Coexpression of Nedd4-1-GFP (left) and hSVCT2-DsRed (middle), and overlaid images (right). Imaging of cotransfected HEK-293 cells occurred at 48h post-transfection.

blot analysis and probed with anti-GFP (can detect YFP) or anti-HA antibodies and the presence of hSVCT2 (Fig. 3Aii) and Nedd4-1 (Fig. 3Aiii) was detected. Next to assess whether this finding translated to observable spatial overlap, we studied hSVCT2 and Nedd4-1 colocalization in HEK-293 cells through confocal microscopy. HEK-293 cells grown on glass-bottomed petri dishes were transiently cotransfected with hSVCT2-DsRed and Nedd4-1-GFP constructs and imaged after 48h. Expectedly, hSVCT2 was localized at the cell membrane as well as in intracellular trafficking structures [33]. Overlay imaging analyses confirmed colocalization between hSVCT2-DsRed and Nedd4-1-GFP in HEK-293 cells (Fig. 3B).

3.4. Effect of coexpression of Nedd4-1 and hSVCT2 on AA uptake in SH-SY5Y cells

As shown in Fig. 4A, coexpression of hSVCT2 and Nedd4-1 displayed a significant ($P<.01$) reduction in 14 C-AA uptake compared to hSVCT2 alone expressing SH-SY5Y cells. In contrast, the coexpression of hSVCT2 and Nedd4-2 did not inhibit the AA transport activity (Fig. 4A). In another study, transfected SH-SY5Y cells expressing Nedd4-1 or Nedd4-2 alone were analyzed for 14 C-AA uptake. No induction of AA uptake was observed upon expression of either of these plasmids in SH-SY5Y cells (Fig. 4B). We also looked

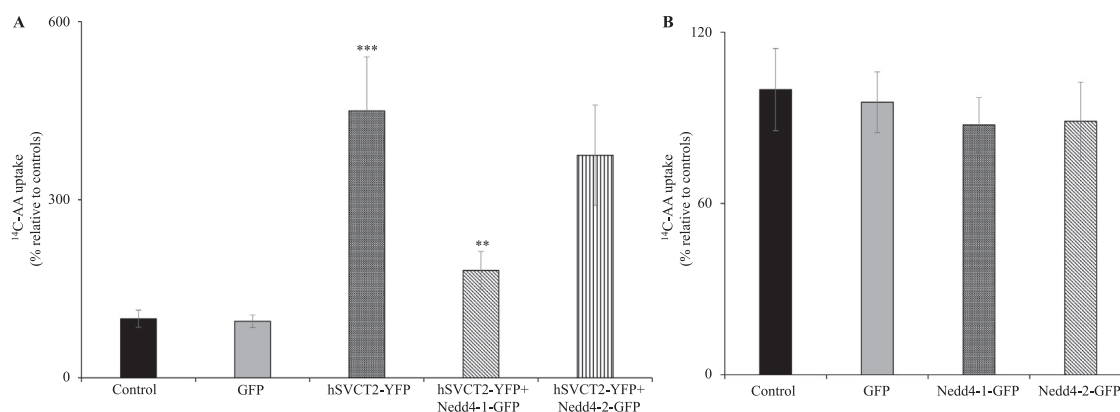


Fig. 4. Effect of Nedd4-1 on hSVCT2 function in SH-SY5Y cells. ¹⁴C-AA uptake was performed in SH-SY5Y cells transiently expressing the indicated constructs (A and B). Data are mean±SEM of at least three separate experiments, with samples collected from different cell passages. ***P*<.01 (decreased compared to hSVCT2-YFP); ****P*<.001 (increased compared to control).

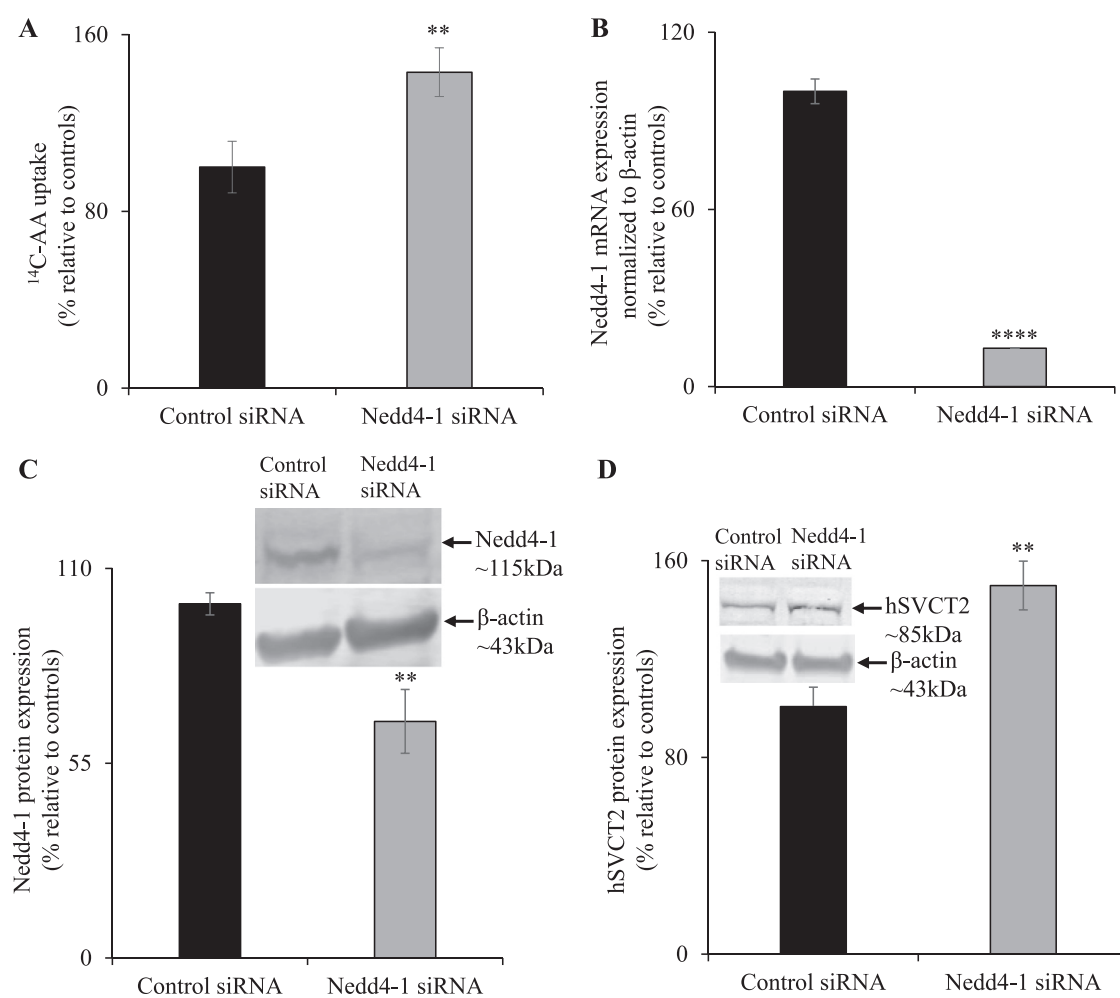


Fig. 5. Effect of knocking down Nedd4-1 via siRNA on ¹⁴C-AA uptake in HEK-293 cells. Effect of knocking down Nedd4-1 on ¹⁴C-AA uptake analysis (A), the expression of Nedd4-1 mRNA by RT-qPCR (B), Nedd4-1 (C) and hSVCT2 (D) protein expression by Western blotting in HEK-293 cells. Cells were processed at 48h post-transfection with either Nedd4-1 siRNA or control (scrambled) siRNA. Data are mean±SEM of at least three separate experimental runs using multiple passages of cells. ***P*<.01; *****P*<.0001.

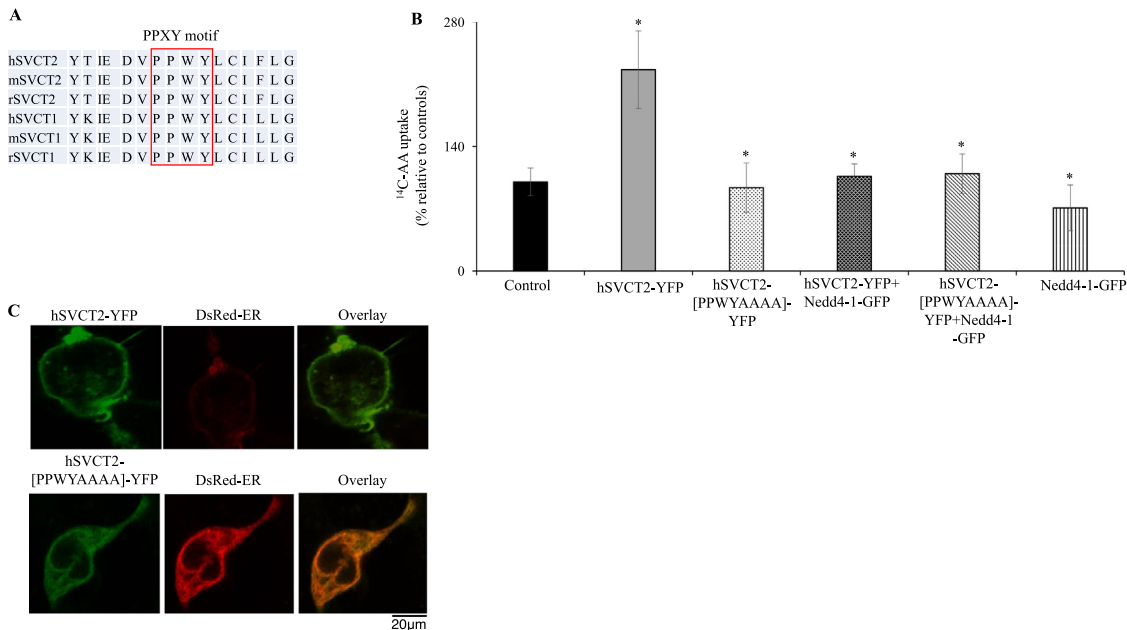


Fig. 6. Effect of hSVCT2 [PPWYAAAA] mutation on the transporter functional expression in HEK-293 cells. (A) Amino acid sequence alignment by clustalW shows the “PPXY” motif is conserved across species and SVCT isoforms. (B) ¹⁴C-AA uptake was performed in HEK-293 cells transiently expressing the indicated constructs. Data are mean ± SEM of at least three separate experiments with multiple determinations. (C) Coexpression of hSVCT2-YFP (WT) or hSVCT2-[PPWYAAAA]-YFP (left) and DsRed-ER (middle), and overlaid images (right). Imaging of cotransfected HEK-293 cells occurred at 48h post-transfection. * $P < .05$.

at the effect on AA uptake from coexpressing hSVCT2 and Nedd4-1 in HEK-293 cells and the results were found to be similar to SH-SY5Y cells (Fig. 6).

3.5. Effect of siRNA knockdown of Nedd4-1 on AA uptake in HEK-293 cells

We examined the effect of silencing the native expression of Nedd4-1 on ¹⁴C-AA uptake. Nedd4-1 siRNA transfected HEK-293 cells displayed a significantly ($P < 0.01$) increased ¹⁴C-AA uptake compared to control (scrambled) siRNA (Fig. 5A). To determine the efficiency of the siRNA knockdown, the Nedd4-1 siRNA and control (scrambled) siRNA transfected HEK-293 cells were subjected to RT-qPCR and Western blot analysis, which showed significantly lower Nedd4-1 mRNA and protein expression levels in the Nedd4-1 siRNA transfected cells (Fig. 5B and C). Conversely, hSVCT2 protein expression was significantly increased in the Nedd4-1 siRNA transfected cells compared with the control (scrambled) siRNA transfected cells (Fig. 5D).

3.6. Effect of hSVCT2-PPXY mutant on AA uptake in HEK-293 cells

Previous studies showed the importance of the classical Nedd4 protein interacting motif (“PPXY”) to the functional expression of other transporters [14,26]. Therefore, we investigated the importance of this motif (“PPXY”, where X can be any amino acid) on AA uptake in HEK-293 cells. This motif (“PPXY”) is present in SVCT transporter isoforms and is conserved across species (human, rat, and mouse; Fig. 6A). First, we mutated hSVCT2 PPWY to AAAA (alanine, neutral amino acid) and the mutated construct alone or together with Nedd4-1 was transfected into HEK-293 cells. As shown in Fig. 6B, the hSVCT2-[PPWYAAAA]-YFP displayed inhibition in ¹⁴C-AA uptake that was significant ($P < .05$) when compared to hSVCT2-YFP (wild-type) expressing HEK-293 cells. In addition, we obtained similar results either with hSVCT2-YFP + Nedd4-1-GFP or hSVCT2-[PPWYAAAA]-YFP + Nedd4-1-GFP coexpressing

HEK-293 cells (Fig. 6B). Further, we determined whether this inhibition was caused by impaired cell surface expression of the transporter or by loss of transporter function. To address this issue, we performed live cell confocal imaging analysis on HEK-293 cells expressing hSVCT2-YFP (wild-type) or hSVCT2-[PPWYAAAA]-YFP separately. Our results showed that the hSVCT2-[PPWYAAAA]-YFP construct displayed an intracellular localization, mainly in endoplasmic reticulum (ER) compared to the observed cell surface expression of the hSVCT2-YFP (wild-type) construct (Fig. 6C). These findings demonstrate that mutating a classical Nedd4 “PPXY” interacting motif within the hSVCT2 polypeptide impairs the cell surface expression of the hSVCT2, and Nedd4-1 is not interacting through this motif to regulate the hSVCT2 function.

3.7. Proteasomal degradation pathway is involved in hSVCT2 functional expression in SH-SY5Y cells

To determine whether reduction in hSVCT2 expression due to ubiquitination can be reversed by proteasome inhibition, proteasome inhibitor (10µM MG132) was used to treat the neuronal cells and then AA uptake and hSVCT2 protein expression were determined at 24h post-treatment. The results demonstrated that ¹⁴C-AA uptake significantly ($P < .05$) increased in MG132 treated compared to untreated SH-SY5Y cells (Fig. 7A) and this upregulation was associated with significantly ($P < .01$) increased hSVCT2 protein expression (Fig. 7B).

4. Discussion

The ubiquitin-proteasomal protein degradation system is involved in regulating the functional expression of several membrane transporters in many cellular systems. To date, the extent of the ubiquitin-proteasomal pathway’s role in modulating hSVCT2 functional expression in neuronal cells remains an unexplored area of study. We addressed this important issue in the current investigation. Previous studies have pointed out that Nedd4-1 plays a vital

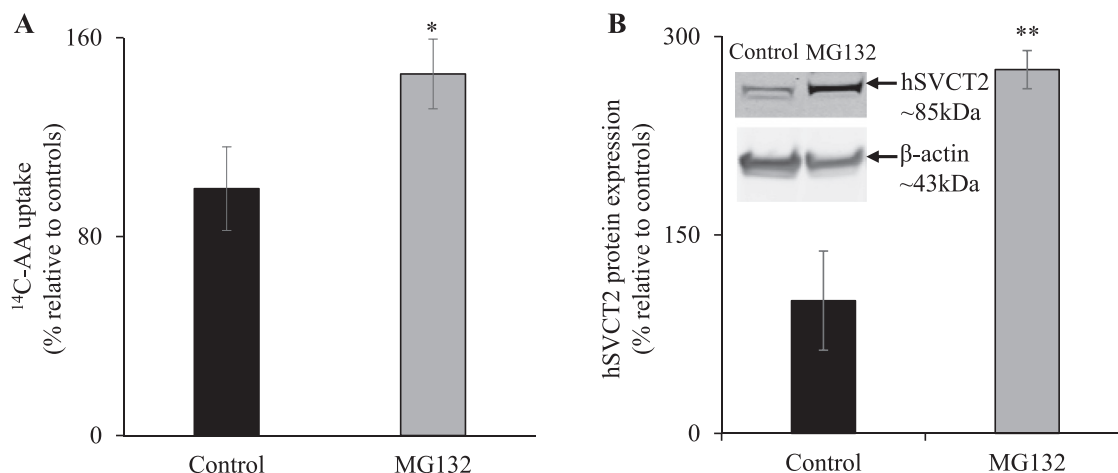


Fig. 7. Effect of proteasomal inhibitor on ¹⁴C-AA uptake and hSVCT2 expression in SH-SY5Y cells. SH-SY5Y cells were treated with MG132 (10 μ M) for 24h and ¹⁴C-AA uptake was performed (A). hSVCT2 protein expression was determined in MG132 treated SH-SY5Y cells by Western blotting (B). Data are mean \pm SEM of at least three independent experimental runs, with samples collected from multiple passages of cells. * P <.05; ** P <.01.

role in neuronal development [18,19] and its importance in neurodegeneration has been increasingly documented in the literature [20–25]. Our findings showed that Nedd4-1 increased in both human AD patient and J20 mouse (age-dependently) hippocampus, which is similar to previous findings in neurodegenerative conditions [25]. The understanding is that Nedd4-1 is typical of a disease protective response to safeguard against accumulation of potentially toxic proteins and thereby defend against the pathogenesis of neurological diseases. However, the increase in Nedd4-1 during AD probably has other potentially detrimental effects such as decreasing the expression of SVCT2 and consequently inhibiting AA uptake in the brain. In addition, previous studies have shown that AD patients present with low vitamin C levels as well as reduced SVCT2 expression. A survey of the literature also suggests that maintaining a normal vitamin C homeostasis yields protective effects that combat age-related cognitive decline and neurodegenerative conditions [1,28]. Our results showed that increased expression of Nedd4-1 inhibits the uptake of AA and decreased expression of Nedd4-1 increased the AA uptake in neuronal and epithelial cells. These data indicate that ubiquitination via Nedd4-1 regulates hSVCT2 functional expression in neuronal and epithelial cells.

The classical Nedd4 protein interacting motif (“PPXY”) is reported to have a fundamental role in regulatory networks of other membrane transporters functional expression [14,26]. Mutating this motif (“PPWY” into “AAAA”) in the hSVCT2 polypeptide led to inhibition of AA uptake (Fig. 6B). This inhibition was caused due to the retention of the transporter intracellularly (Fig. 6C). However, this finding demonstrates that the effect of Nedd4-1 on hSVCT2 functional expression could occur via binding to other motifs or regions along the hSVCT2 polypeptide, or interaction with non-classical interacting motifs as shown by others [12,34,35]. Future studies will address these possibilities.

Overall, our study provides the first evidence demonstrating a role for the ubiquitin-proteasomal protein degradation pathway involved in regulating the functional expression of hSVCT2 in neuronal and epithelial cells that subsequently impacts the AA uptake under physiological and pathophysiological conditions relevant to neurodegenerative diseases.

Data availability

All data generated or analyzed during this study are included in this published article.

Declaration of competing interest

The authors have read the journal’s policy on disclosing potential conflicts of interest, and they all declare no personal or financial conflict of interest.

CRediT authorship contribution statement

Trevor Teafatiller: Validation, Formal analysis, Methodology, Investigation, Visualization, Writing – original draft, Writing – review & editing. **Oasis Perez:** Formal analysis, Methodology, Visualization, Writing – review & editing. **Masashi Kitazawa:** Methodology, Resources, Writing – review & editing. **Anshu Agrawal:** Conceptualization, Resources, Writing – original draft, Writing – review & editing. **Veedamali S. Subramanian:** Conceptualization, Validation, Formal analysis, Methodology, Investigation, Visualization, Writing – original draft, Writing – review & editing, Project administration, Supervision, Resources, Funding acquisition.

Acknowledgements

This work was supported by the National Institutes of Health (DK-107474 and DK-107474S1 to VSS). The University of California, Irvine, Alzheimer’s Disease Research Center (UCI ADRC) is funded by NIH/NIA Grant P30AG066519 (previously P50 AG16573).

References

- [1] Harrison FE. A critical review of vitamin C for the prevention of age-related cognitive decline and Alzheimer’s disease. *J Alzheimers Dis* 2012;29:711–26.
- [2] Monacelli F, Acquarone E, Giannotti C, Borghi R, Nencioni A. Vitamin C, aging and Alzheimer’s disease. *Nutrients* 2017;9:670.
- [3] May JM. Vitamin C transport and its role in the central nervous system. *Subcell Biochem* 2012;56:85–103.
- [4] Bürzle M, Suzuki Y, Ackermann D, Miyazaki H, Maeda N, Cléménçon B, et al. The sodium-dependent ascorbic acid transporter family SLC23. *Mol Aspects Med* 2013;34:436–54.
- [5] Qiu S, Li L, Weeber EJ, May JM. Ascorbate transport by primary cultured neurons and its role in neuronal function and protection against excitotoxicity. *J Neurosci Res* 2007;85:1046–56.
- [6] Subramanian VS, Teafatiller T, Agrawal A, Kitazawa M, Marchant JS. Effect of lipopolysaccharide and TNF α on neuronal ascorbic acid uptake. *Mediators Inflamm* 2021;2021:4157132.
- [7] Medina AB, Banaszczak M, Ni Y, Aretz I, Meierhofer D. ρ^0 cells feature de-ubiquitination of SLC transporters and increased levels and fluxes of amino acids. *Int J Mol Sci* 2017;18:879.
- [8] Weber J, Polo S, Maspero E. HECT E3 ligases: a tale with multiple facets. *Front Physiol* 2019;10:370.

- [9] van Wijk SJ, Fulda S, Dikic I, Heilemann M. Visualizing ubiquitination in mammalian cells. *EMBO Rep* 2019;20:e46520.
- [10] Komander D, Rape M. The ubiquitin code. *Annu Rev Biochem* 2012;81:203–29.
- [11] Rotin D, Staub O. Role of the ubiquitin system in regulating ion transport. *Pflugers Arch* 2011;461:1–21.
- [12] Xu D, Wang H, Gardner C, Pan Z, Zhang PL, Zhang J, et al. The role of Nedd4-1 WW domains in binding and regulating human organic anion transporter 1. *Am J Physiol Renal Physiol* 2016;311:F320–9.
- [13] Xia X, Roundtree M, Merikhi A, Lu X, Shentu S, Lesage G. Degradation of the apical sodium-dependent bile acid transporter by the ubiquitin-proteasome pathway in cholangiocytes. *J Biol Chem* 2004;279:44931–7.
- [14] Bobby R, Medini K, Neudecker P, Lee TV, Brimble MA, McDonald FJ, et al. Structure and dynamics of human Nedd4-1 WW3 in complex with the α ENaC PY motif. *Biochim Biophys Acta* 2013;1834:1632–41.
- [15] Akkaya BG, Zolnerciks JK, Ritchie TK, Bauer B, Hartz AM, Sullivan JA, et al. The multidrug resistance pump ABCB1 is a substrate for the ubiquitin ligase NEDD4-1. *Mol Membr Biol* 2015;32:39–45.
- [16] No YR, He P, Yoo BK, Yun CC. Unique regulation of human Na⁺/H⁺ exchanger 3 (NHE3) by Nedd4-2 ligase that differs from non-primate NHE3s. *J Biol Chem* 2014;289:18360–72.
- [17] Henry PC, Kanelis V, O'Brien MC, Kim B, Gautschi I, Forman-Kay J, et al. Affinity and specificity of interactions between Nedd4 isoforms and the epithelial Na⁺ channel. *J Biol Chem* 2003;278:20019–28.
- [18] Hsia HE, Kumar R, Luca R, Takeda M, Courchet J, Nakashima J, et al. Ubiquitin E3 ligase Nedd4-1 acts as a downstream target of PI3K/PTEN-mTORC1 signaling to promote neurite growth. *Proc Natl Acad Sci U S A* 2014;111:13205–10.
- [19] Kawabe H, Neeb A, Dimova K, Young SM Jr, Takeda M, Katsurabayashi S, et al. Regulation of Rap2A by the ubiquitin ligase Nedd4-1 controls neurite development. *Neuron* 2010;65:358–72.
- [20] Sugeno N, Hasegawa T, Tanaka N, Fukuda M, Wakabayashi K, Oshima R, et al. Lys-63-linked ubiquitination by E3 ubiquitin ligase Nedd4-1 facilitates endosomal sequestration of internalized α -synuclein. *J Biol Chem* 2014;289:18137–51.
- [21] Xing LF, Guo HP, Wang DT, Sun LH, Pan SY. Protective effects and mechanisms of Ndfip1 on SH-SY5Y cell apoptosis in an in vitro Parkinson's disease model. *Genet Mol Res* 2016;15:gmr6963.
- [22] Zhang Y, Guo O, Huo Y, Wang G, Man HY. Amyloid- β induces AMPA receptor ubiquitination and degradation in primary neurons and human brains of Alzheimer's disease. *J Alzheimers Dis* 2018;62:1789–801.
- [23] Zhang H, Nie W, Zhang X, Zhang G, Li Z, Wu H, et al. NEDD4-1 regulates migration and invasion of glioma cells through CNrasGEF ubiquitination in vitro. *PLoS One* 2013;8:e82789.
- [24] Rodrigues EM, Scudder SL, Goo MS, Patrick GN. $A\beta$ -Induced synaptic alterations require the e3 ubiquitin ligase Nedd4-1. *J Neurosci* 2016;36:1590–5.
- [25] Kwak YD, Wang B, Li JJ, Wang R, Deng Q, Diao S, et al. Upregulation of the E3 ligase NEDD4-1 by oxidative stress degrades IGF-1 receptor protein in neurodegeneration. *J Neurosci* 2012;32:10971–81.
- [26] Zhou R, Patel SV, Snyder PM. Nedd4-2 catalyzes ubiquitination and degradation of cell surface ENaC. *J Biol Chem* 2007;282:20207–12.
- [27] Persaud A, Alberts P, Amsen EM, Xiong X, Wasmuth J, Saadon Z, et al. Comparison of substrate specificity of the ubiquitin ligases Nedd4 and Nedd4-2 using proteome arrays. *Mol Syst Biol* 2009;5:333.
- [28] Subramanian VS, Teafatiller T, Vidal J, Gunaratne GS, Rodriguez-Ortiz CJ, Kitazawa M, et al. Calsyntenin-3 interacts with the sodium-dependent vitamin C transporter-2 to regulate vitamin C uptake. *Int J Biol Macromol* 2021;192:1178–84.
- [29] Malik B, Schlanger L, Al-Khalili O, Bao HF, Yue G, Price SR, et al. Enac degradation in A6 cells by the ubiquitin-proteasome proteolytic pathway. *J Biol Chem* 2001;276:12903–10.
- [30] Malhotra P, Soni V, Yamanashi Y, Takada T, Suzuki H, Gill RK, et al. Mechanisms of Niemann-Pick type C1 Like 1 protein degradation in intestinal epithelial cells. *Am J Physiol Cell Physiol* 2019;316:C559–66.
- [31] Mucke L, Masliah E, Yu GQ, Mallory M, Rockenstein EM, Tatsuno G, et al. High-level neuronal expression of abeta 1–42 in wild-type human amyloid protein precursor transgenic mice: synaptotoxicity without plaque formation. *J Neurosci* 2000;20:4050–8.
- [32] Heskett CW, Teafatiller T, Hennessey C, Gareau MG, Marchant JS, Said HM, et al. Enteropathogenic escherichia coli infection inhibits intestinal ascorbic acid uptake via dysregulation of its transporter expression. *Dig Dis Sci* 2020;66:2250–60.
- [33] Subramanian VS, Marchant JS, Said HM. Molecular determinants dictating cell surface expression of the human sodium-dependent vitamin C transporter-2 in human liver cells. *Am J Physiol Gastrointest Liver Physiol* 2010;298:G267–74.
- [34] Shenoy SK, Xiao K, Venkataramanan V, Snyder PM, Freedman NJ, Weissman AM. Nedd4 mediates agonist-dependent ubiquitination, lysosomal targeting, and degradation of the beta2-adrenergic receptor. *J Biol Chem* 2008;283:22166–76.
- [35] Simonin A, Fuster D. Nedd4-1 and beta-arrestin-1 are key regulators of Na⁺/H⁺ exchanger 1 ubiquitylation, endocytosis, and function. *J Biol Chem* 2010;285:38293–303.